

# IAML: Illumination-Aware Mirror Loss for Progressive Learning in Low-Light Image Enhancement Auto-encoders

Farida Mohsen, Tala Zaim, Ali Al-Zawqari, Ali Safa, *Member, IEEE*, and Samir Belhaouari, *Senior Member, IEEE*

**Abstract**—This letter presents a novel training approach and loss function for learning low-light image enhancement auto-encoders. Our approach revolves around the use of a teacher-student auto-encoder setup coupled to a progressive learning approach where multi-scale information from clean image decoder feature maps is distilled into each layer of the student decoder in a mirrored fashion using a newly-proposed loss function termed **Illumination-Aware Mirror Loss (IAML)**. IAML helps aligning the feature maps within the student decoder network with clean feature maps originating from the teacher side while taking into account the effect of lighting variations within the input images. Extensive benchmarking of our proposed approach on three popular low-light image enhancement datasets demonstrate that our model achieves state-of-the-art performance in terms of average SSIM, PSNR and LPIPS reconstruction accuracy metrics. Finally, ablation studies are performed to clearly demonstrate the effect of IAML on the image reconstruction accuracy.

**Index Terms**—Low-light image enhancement, auto-encoders, loss function design.

## I. INTRODUCTION

IN the past decade, low-light image enhancement using modern deep learning (DL) techniques has been an active area of research, with applications to nighttime vision for autonomous car navigation, remote sensing, photography enhancement and so on [1], [2], [3], [4], [5]. The use of DL models over traditional luminosity and exposure amplification has constituted a major leap forward within the field, enabling much higher fidelity image recovery even within extreme low-light conditions where conventional luminosity and exposure manipulation fails [6], [7], [8], [9].

Within this context, the use of convolutional *auto-encoder* architectures has been widely adopted as one of the models of choice for low-light image enhancement [6]. Certainly, auto-encoders constitute a natural choice for this application following their ability at reconstructing output images of the same type and dimension as their input image [10]. Furthermore, the use of *skip connections* [11], where the original input image is added as an additional input to subsequent layers, has also been proven to be critical for achieving high-accuracy image

reconstruction. Popular models such as the U-Net architecture have therefore been utilized in many works related to image restoration, as a well-suited auto-encoder backbone equipped with skip connections and moderate compute complexity [12].

In addition to DL architectural choices, the choice of the *loss function* used during training has been proven to be of crucial importance [13]. Indeed, prior works have explored how the design of the loss function impacts the performance of low-light image enhancement models [13], in terms of standard benchmark metrics such as *Structural Similarity Index Measure* (SSIM), *Peak Signal-to-Noise Ratio* (PSNR) and *Learned Perceptual Image Patch Similarity* (LPIPS) [14], [15].

Following these realizations within the field, this paper focuses on the design of a novel loss function termed *Illumination-Aware Mirror Loss* (IAML) for learning low-light enhancement auto-encoder models. Inspired by the growing use of teacher-student setups [16], our proposed IAML loss is used alongside a custom teacher-student auto-encoder setup that distills information from clean image representations into each layer of the student's decoder sub-network, better guiding model learning during the training procedure. The contributions of this paper are the following:

- 1) We introduce a teacher-student paradigm for low-light image enhancement where the teacher processes clean images while the student enhances degraded ones, enabling implicit learning of clean image priors.
- 2) We propose a novel IAML loss that aligns student decoder feature maps with clean teacher decoder ones across all layers, facilitating multi-scale feature learning and distillation.
- 3) We perform extensive benchmarking and ablation studies to clearly demonstrating the usefulness of IAML and we show that our proposed approach outperforms more than a dozen prior techniques on three popular benchmark datasets.

This paper is organized as follows. The proposed methods are introduced in Section II. Experimental studies are presented in Section III. Finally, conclusions are provided in Section IV.

## II. PROPOSED METHOD

This section describes our proposed method for low-light image enhancement, based on the formulation of a multi-level mirror learning scheme between a *teacher* encoder network

F. Mohsen, T. Zaim, A. Safa and S. Belhaouari are with the College of Science and Engineering, Hamad Bin Khalifa University, Doha, Qatar. emails: {fmohsen, taza89388, asafa, sbelhaouari}@hbku.edu.qa;

A. Al-Zawqari is with the ELEC department, Vrije Universiteit Brussel, Brussels, Belgium. emails: ali.mohammed.mohammed.al-zawqari@vub.be;

F. Mohsen developed the methods and performed the experiments. T. Zaim and A. Al-Zawqari contributed to the analysis of the results. A. Safa and S. Belhaouari supervised the project as Principal Investigators. All authors contributed to the writing of the manuscript.

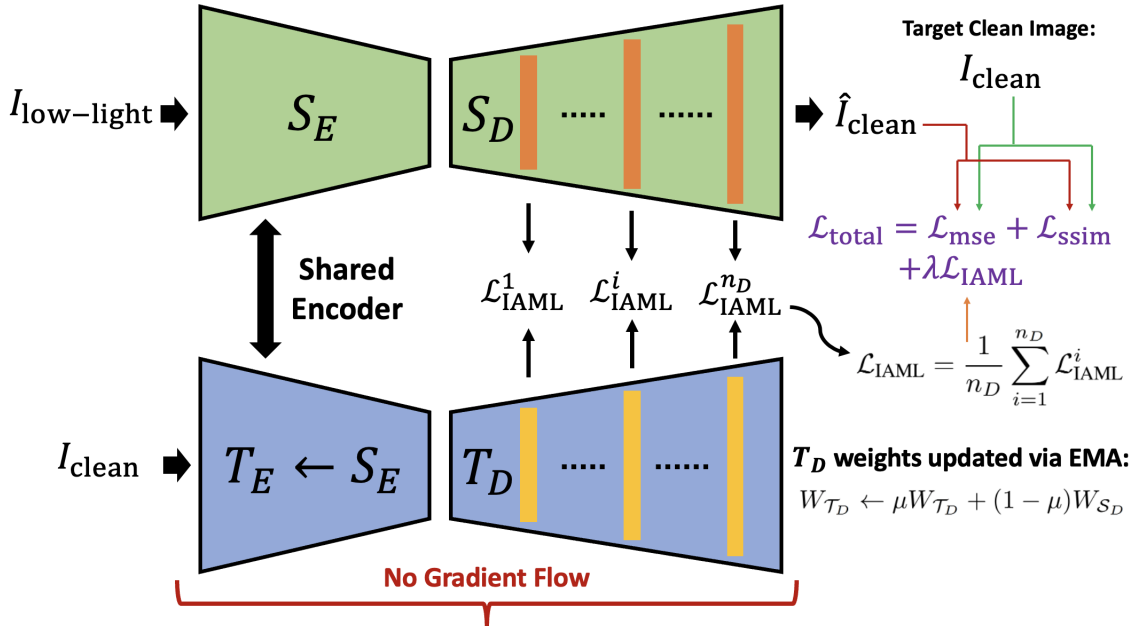


Fig. 1. Proposed teacher-student auto-encoder setup for low-light image enhancement. The student network  $\mathcal{S}$  receives as input the degraded low-light images  $I_{\text{low-light}}$  and seeks to recover the clean images  $\hat{I}_{\text{clean}}$ . The teacher network  $\mathcal{T}$  shares the same encoder as  $\mathcal{S}$  (updated as  $\mathcal{T}_E \leftarrow \mathcal{S}_E$  during the training iterations) and updates its decoder  $\mathcal{T}_D$  via an exponential moving average using the weights of the student decoder  $\mathcal{S}_D$  (no gradient-based learning in  $\mathcal{T}$ ). The teacher takes as input the clean target images  $I_{\text{clean}}$ , leading to clean multi-scale feature maps at each layer of  $\mathcal{T}_D$ . These clean feature maps are then used to guide the learning of the layers within  $\mathcal{S}_D$  in a mirrored fashion using the proposed Illumination-Aware Mirror Loss (IAML).

and a *student* auto-encoder which learns to output the enhanced image from the degraded low-light input image.

#### A. Teacher-student auto-encoder setup

Our proposed neural network setup is composed of both a teacher and a student auto-encoder, as shown in Fig. 1. First, we set up a *student* auto-encoder  $\mathcal{S}$  which always takes as input the degraded low-light images  $I_{\text{low-light}}$  and aims to reconstruct the corresponding target clean images  $I_{\text{clean}}$ .

$$\min \|\hat{I}_{\text{clean}} - I_{\text{clean}}\|_2 \text{ given } \hat{I}_{\text{clean}} = \mathcal{S}(I_{\text{low-light}}) \quad (1)$$

We respectively denote by  $\mathcal{S}_E$  and  $\mathcal{S}_D$  the encoder and decoder parts of  $\mathcal{S}$ . Then, in addition to the student auto-encoder, we set up a *teacher* auto-encoder  $\mathcal{T}$  which strictly takes as input the target clean images  $I_{\text{clean}}$  and seeks to reproduce them as its output. Crucially, the encoder part of  $\mathcal{T}$  noted  $\mathcal{T}_E$  is an exact copy of the student encoder  $\mathcal{S}_E$  (shared encoder), with the difference that the backpropagation of gradients is *disabled* so that the clean images given as input to the teacher encoder  $\mathcal{T}_E$  never impact the learning of this shared encoder block:

$$\mathcal{T}_E \leftarrow \mathcal{S}_E \quad (2)$$

Now, regarding the teacher decoder  $\mathcal{T}_D$ , both the student and teacher encoders are initialized with the same random weights at the beginning of the training process:

$$\mathcal{T}_D^0, \mathcal{S}_D^0 \leftarrow \text{random init} \quad (3)$$

Then, during the learning process, gradients are allowed to flow within the *student* decoder while being *blocked* for the *teacher* decoder once again. Instead, at each learning iteration,

the teacher decoder  $\mathcal{T}_D$  is updated following an *exponential moving average* (EMA) scheme as follows [17]:

$$W_{T_D} \leftarrow \mu W_{T_D} + (1 - \mu) W_{S_D} \quad (4)$$

where  $\mu$  is the EMA coefficient,  $W_{T_D}$  denotes the teacher decoder weights and  $W_{S_D}$  denotes the student decoder weights (where gradient-based update occurs). During training, the multi-scale feature representations within  $\mathcal{S}_D$  will undergo an *alignment* process with regard to the representations within  $\mathcal{T}_D$ , corresponding to feature maps associated with the clean target images  $I_{\text{clean}}$  that the student need to produce. This is done through the formulation of a novel loss function strategy, which will be explained in Section II-B.

The combination of the shared encoder  $\mathcal{S}_E = \mathcal{T}_E$  processing both the degraded low-light and clean inputs, together with the EMA-driven teacher decoder  $\mathcal{T}_D$  creates a *self-distillation loop*: the teacher receives as input images in the clean domain and gradually converges to produce *ideal* intermediate representations, which the student processing within the degraded domain is trained to mirror. The EMA-based update of  $\mathcal{T}_D$  ensures smooth, non-collapsing targets. Gradient stopping prevents the teacher from being directly optimized, preserving the asymmetric role of the two branches.

#### B. Illumination-aware mirror loss

The goal of our proposed IAML is to force each feature map produced within  $\mathcal{S}_D$  to align itself with the corresponding feature map of  $\mathcal{T}_D$  which processes the target clean images. Doing so, layer-wise and *multi-scale* information about the feature representations of clean images are injected at each scale level of  $\mathcal{S}_D$ , better guiding it during learning towards

the generation of clean images from its degraded low-light inputs.

Crucially, our proposed mirror loss is made *illumination-aware*. Indeed, because the student and teacher model decode features from two different illumination domains, their intermediate activations occupy different dynamic ranges. Hence, a naive  $\ell_1$  or  $\ell_2$  matching between corresponding student and teacher feature maps would be dominated by domain-level magnitude differences rather than structural discrepancies.

To alleviate this, we adopt a *weighted loss* approach taking into account the luminance of each pixel in the input images as follows. Given the low-light input  $I_{\text{low-light}}$ , we compute a luminance map  $L_{\mathbf{p}}$  per pixel  $\mathbf{p}$  via the standard RGB-to-luminance coefficients [18]:

$$L_{\mathbf{p}} = 0.299 I_{\text{low-light},\mathbf{p}}^R + 0.587 I_{\text{low-light},\mathbf{p}}^G + 0.114 I_{\text{low-light},\mathbf{p}}^B \quad (5)$$

Then,  $L_{\mathbf{p}}$  is min-max normalized to  $\tilde{L}_{\mathbf{p}} \in [0, 1]$ , and converted to an *emphasis weight matrix*:

$$W_{\mathbf{p}} = 1 + \beta (1 - \tilde{L}_{\mathbf{p}}), \quad \beta = 0.6, \quad (6)$$

so that darker regions receive weight up to  $1 + \beta = 1.6$  while well-lit regions receive the base weight of 1.0. Later on, upon feeding an input sample, its corresponding  $W_{\mathbf{p}}$  can be resized to match the size of each feature scale  $i$ , noted as  $W^i$ .

In addition, we first apply *standard normalization* to the *flattened* student and teacher feature maps  $f_S^i, f_T^i$  for all decoder scale levels  $i$  as follows:

$$\tilde{f}_{S,T}^i \leftarrow \frac{\tilde{f}_{S,T}^i - \mu(\tilde{f}_{S,T}^i)}{\sigma(\tilde{f}_{S,T}^i + \epsilon)}, \quad \epsilon = 10^{-6}, \quad (7)$$

where  $\mu$  and  $\sigma$  respectively denote the mean and standard deviation operators (and  $\epsilon$  avoids division by zero). Doing so, the proposed IAML at decoder layer level  $i$  is then defined as:

$$\mathcal{L}_{\text{IAML}}^i = \left\langle W^i \odot | \tilde{f}_S^i - \text{sg}(\tilde{f}_T^i) | \right\rangle, \quad (8)$$

where  $\langle \cdot \rangle$  denotes spatial averaging,  $\odot$  is the element-wise multiplication with broadcasting over the channel dimension and  $\text{sg}(\cdot)$  denotes the blocking of the gradient flow associated with the teacher data. Finally, the total IAML is computed as the average across all decoder levels  $i = 1, \dots, n_D$ :

$$\mathcal{L}_{\text{IAML}} = \frac{1}{n_D} \sum_{i=1}^{n_D} \mathcal{L}_{\text{IAML}}^i. \quad (9)$$

### C. Global loss function

During training, the final loss is computed as a combination of a per-pixel reconstruction loss and the proposed IAML:

$$\mathcal{L}_{\text{total}} = \underbrace{\mathcal{L}_{\text{mse}} + \mathcal{L}_{\text{ssim}}}_{\text{per-pixel reconstruction}} + \underbrace{\lambda \mathcal{L}_{\text{IAML}}}_{\text{feature map distillation}} \quad (10)$$

where  $\mathcal{L}_{\text{mse}}$  is the standard mean square error between the student decoder output  $\hat{I}_{\text{clean}}$  and the target clean image  $I_{\text{clean}}$ ,  $\mathcal{L}_{\text{ssim}} = 1 - \text{SSIM}(\hat{I}_{\text{clean}}, I_{\text{clean}})$  is the *structural similarity* loss [13] and  $\lambda$  is a hyper-parameter defining the strength of the proposed IAML contribution.

TABLE I  
QUANTITATIVE COMPARISON OF METHODS ON THE LOL-V1 DATASET.  
BEST SCORES ARE IN BOLD.

Method	SSIM $\uparrow$	PSNR $\uparrow$	LPIPS $\downarrow$
LIME [19]	0.564	16.74	0.350
SRIE [20]	15.12	0.569	0.340
BVIF [21]	0.561	16.61	0.286
BIMEF [22]	0.566	14.80	0.326
ZeroDCE++ [23]	0.595	16.72	0.335
EnlightenGAN [24]	0.650	17.48	0.322
RetinexNet [25]	0.560	16.77	0.474
KinD [26]	0.790	20.86	0.207
MIRNet [27]	0.830	<b>24.14</b>	0.131
UFormer [28]	0.771	16.36	0.321
Restormer [29]	0.823	22.43	0.141
LANet [30]	0.810	21.71	0.101
SurroundNet [1]	0.853	23.84	0.113
Retinexformer [2]	0.816	23.69	0.140
SCFR-WLMB [31]	0.811	23.270	–
LightenDiffusion [32]	0.811	19.977	0.178
<b>IAML (ours)</b>	<b>0.876</b>	<b>23.84</b>	<b>0.0848</b>

## III. EXPERIMENTAL SETUP

### A. Model architecture and training procedure

As auto-encoder backbone, we use the popular U-Net architecture with CBAM attention [33] used at each scale. As detailed in Section II-A, both the student and teacher networks share this same architecture. During training, images are randomly cropped to 256×256 patches with horizontal and vertical flipping augmentation. We use the Adam optimizer with an initial learning rate of  $2 \times 10^{-4}$ ,  $\beta_1 = 0.9$ ,  $\beta_2 = 0.999$ , and a cosine-annealing schedule over 500 epochs with batch size 8. The EMA momentum in (4) is fixed at  $\mu = 0.999$  throughout training. In addition, grid search has been performed on the hyper-parameter  $\lambda$  in (10) and the best results corresponding to  $\lambda = 0.8$  are reported. All experiments are carried using an NVIDIA RTX 4090 GPU.

### B. Benchmark Datasets

We evaluate our proposed approach on three *widely adopted* low-light benchmarks: LOL-v1, LOL-v2-Real and LOL-v2-Synthetic. First, LOL-v1 [25] contains 485 training and 15 test image pairs captured under real low-light conditions. Then, LOL-v2-Real [34] extends the LOL-v1 protocol with 689 training and 100 test pairs captured in real-world settings. Finally, LOL-v2-Synthetic [34] provides 900 training and 100 test pairs generated via synthetic degradation pipelines. All three datasets supply spatially aligned low-light / normal-light pairs enabling supervised training and reliable quantitative evaluation.

### C. Benchmark results

During the benchmarking process, we use three widely used and standard similarity measurement scores: SSIM (the higher the better), PSNR (the higher the better) and LPIPS (the lower the better) [14], [15].

On LOL-v1, our method achieves state-of-the-art perceptual quality, with the highest SSIM and lowest LPIPS metrics

TABLE II  
QUANTITATIVE COMPARISON OF METHODS ON THE LOL-V2-REAL AND LOL-V2-SYNTHETIC DATASETS. BEST SCORES ARE IN BOLD.

Method	LOL-v2-real			LOL-v2-synthetic		
	SSIM $\uparrow$	PSNR $\uparrow$	LPIPS $\downarrow$	SSIM $\uparrow$	PSNR $\uparrow$	LPIPS $\downarrow$
LIME [19]	0.469	15.19	0.415	0.776	16.85	0.675
SRIE [20]	0.556	16.12	0.332	0.617	14.51	0.196
BVIF [21]	0.546	16.43	0.317	0.717	17.24	0.198
BIMEF [22]	0.613	16.51	0.307	0.616	14.09	0.193
ZeroDCE++ [23]	0.571	18.75	0.313	0.829	18.04	0.168
EnlightenGAN [24]	0.617	18.23	0.309	0.734	16.57	0.212
RetinexNet [25]	0.567	15.47	0.365	0.798	17.13	0.754
KinD [26]	0.641	14.74	0.375	0.578	13.29	0.435
MIRNet [27]	0.820	20.02	0.317	0.876	21.94	0.112
UFormer [28]	0.771	18.82	0.347	0.871	19.66	0.107
Restormer [29]	0.827	19.94	0.191	0.830	21.41	0.066
LANet [30]	0.780	19.21	0.178	0.882	22.54	0.069
SurroundNet [1]	0.807	20.18	0.144	0.900	23.88	0.068
Retinexformer [2]	0.814	21.43	0.184	0.930	24.16	0.061
URetinex-Net++ [3]	0.811	20.55	0.143	0.899	24.02	0.067
SCFR-WLMB [31]	0.834	21.430	–	0.917	<b>25.830</b>	–
LightenDiffusion [32]	0.853	<b>22.831</b>	0.167	0.867	21.523	0.157
<b>IAML (ours)</b>	<b>0.855</b>	<u>21.45</u>	<b>0.15</b>	<b>0.932</b>	<u>24.82</u>	<b>0.058</b>

among all compared methods, while reaching second-best position on the PSNR metric (see Table I). Furthermore, Table II reports benchmark metrics on LOL-v2-Real and LOL-v2-Synthetic, clearly showing once again that our method achieves state-of-the-art performance in terms of SSIM and LPIPS, while systematically reaching second-best performance in terms of PSNR.

Overall, when evaluating the average SSIM, PSNR and LPIPS across all datasets, Table III clearly shows that our method outperforms prior approaches by reaching the highest average SSIM, PSNR and LPIPS measures.

TABLE III  
AVERAGE BENCHMARK METRICS ACROSS LOL-V1, LOL-V2-REAL AND LOL-V2-SYNTHETIC.

Method	SSIM $\uparrow$	PSNR $\uparrow$	LPIPS $\downarrow$
LIME [19]	0.603	16.26	0.480
SRIE [20]	5.431	10.40	0.289
BVIF [21]	0.608	16.76	0.267
BIMEF [22]	0.598	15.13	0.275
ZeroDCE++ [23]	0.665	17.84	0.272
EnlightenGAN [24]	0.667	17.43	0.281
RetinexNet [25]	0.642	16.46	0.531
KinD [26]	0.670	16.30	0.339
MIRNet [27]	0.842	22.03	0.187
UFormer [28]	0.804	18.28	0.258
Restormer [29]	0.827	21.26	0.133
LANet [30]	0.824	21.15	0.116
SurroundNet [1]	0.853	22.62	0.098
Retinexformer [2]	0.853	23.09	0.128
SCFR-WLMB [31]	0.854	23.51	–
LightenDiffusion [32]	0.844	21.44	0.167
<b>IAML (ours)</b>	<b>0.888</b>	<b>23.37</b>	<b>0.098</b>

#### D. Ablation studies

Importantly, in order to explore the impact of our proposed IAML approach, we perform ablation studies on the mirror loss formulation in (8) and on the total loss formulated in

TABLE IV  
ABLATION STUDY ON THE EFFECT OF THE LOSS FORMULATION ON THE AVERAGE SSIM, PSNR AND LPIPS. BEST RESULTS ARE SHOWN IN BOLD, AND SECOND-BEST RESULTS ARE UNDERLINED.

Loss Configuration	SSIM $\uparrow$	PSNR $\uparrow$	LPIPS $\downarrow$
1) MSE only	0.8545	23.3342	0.0935
2) MSE + SSIM	0.8722	23.1278	0.0897
3) MSE + SSIM + Cos. Sim.	0.8606	23.3549	0.0989
4) MSE + SSIM + Std. $\ell_1$	<u>0.8737</u>	<u>23.801</u>	<u>0.0882</u>
5) <b>MSE + SSIM + IAML</b>	<b>0.888</b>	<b>23.37</b>	<b>0.098</b>

(10). Table IV reports the SSIM, PSNR and LPIPS metrics for five different ablation cases on our loss formulation. In Table IV, entry 3) replaces the IAML with *cosine similarity* losses between student and teacher decoder feature maps. Furthermore, entry 4) replaces the IAML with an  $\ell_1$  loss between standardized student and teacher decoder feature maps (7). Finally, entry 5) denotes our full IAML approach. Table IV clearly demonstrates that our custom IAML formulation (entry 5) leads to the best performance, showing the crucial effect of illumination-aware feature map distillation during training.

#### IV. CONCLUSION

This paper has presented a novel method for the training of low-light image enhancement auto-encoders. The proposed IAML framework relies on a teacher-student pair of auto-encoder network where information from teacher feature maps corresponding to clean input image representations are used to guide the training of the student model, by aligning the student decoder’s internal representations with the teacher ones. Extensive benchmarking and ablation studies have clearly demonstrated the usefulness of our approach, outperforming more than a dozen prior methods in terms of average SSIM, PSNR and LPIPS across three datasets. As future work, we plan to apply our approach to other image restoration tasks in order to study its validity across various application domains.

## REFERENCES

- [1] F. Zhou, X. Sun, J. Dong, and X. Zhu, "Surroundnet: Towards effective low-light image enhancement," *Pattern Recognition*, vol. 141, p. 109602, 2023.
- [2] Y. Cai, H. Bian, J. Lin, H. Wang, R. Timofte, and Y. Zhang, "Retinex-former: One-stage retinex-based transformer for low-light image enhancement," in *ICCV*, 2023, pp. 12 504–12 513.
- [3] W. Wu, J. Weng, P. Zhang, X. Wang, W. Yang, and J. Jiang, "Interpretable optimization-inspired unfolding network for low-light image enhancement," *IEEE Transactions on Pattern Analysis and Machine Intelligence*, 2025.
- [4] Q. Xiao, H. Jin, H. Su, and R. Yan, "Sell:a method for low-light image enhancement by predicting semantic priors," *IEEE Signal Processing Letters*, vol. 32, pp. 1785–1789, 2025.
- [5] J. He, S. Palaiahnakote, A. Ning, and M. Xue, "Zero-shot low-light image enhancement via joint frequency domain priors guided diffusion," *IEEE Signal Processing Letters*, vol. 32, pp. 1091–1095, 2025.
- [6] C. Li, C. Guo, L. Han, J. Jiang, M.-M. Cheng, J. Gu, and C. C. Loy, "Low-light image and video enhancement using deep learning: A survey," *IEEE Transactions on Pattern Analysis and Machine Intelligence*, vol. 44, no. 12, pp. 9396–9416, 2022.
- [7] Z.-M. Du, H.-A. Li, and F.-l. Han, "Dynamic fusion for generating high-quality labels in low-light image enhancement," *IEEE Signal Processing Letters*, vol. 32, pp. 2324–2328, 2025.
- [8] H. Lee, K. Sohn, and D. Min, "Unsupervised low-light image enhancement using bright channel prior," *IEEE Signal Processing Letters*, vol. 27, pp. 251–255, 2020.
- [9] J. Kim, G.-H. Park, J. Bae, and S.-W. Jung, "Intrinsic decomposition-based curriculum learning for low-light image enhancement," *IEEE Signal Processing Letters*, vol. 32, pp. 4019–4023, 2025.
- [10] A. Safa, T. Verbelen, O. Çatal, T. Van de Maele, M. Hartmann, B. Dhoedt, and A. Bourdoux, "Fmcw radar sensing for indoor drones using variational auto-encoders," in *2023 IEEE Radar Conference (RadarConf23)*, 2023, pp. 1–6.
- [11] K. He, X. Zhang, S. Ren, and J. Sun, "Deep residual learning for image recognition," in *2016 IEEE Conference on Computer Vision and Pattern Recognition (CVPR)*, 2016, pp. 770–778.
- [12] O. Ronneberger, P. Fischer, and T. Brox, "U-net: Convolutional networks for biomedical image segmentation," in *Medical Image Computing and Computer-Assisted Intervention – MICCAI 2015*, N. Navab, J. Hornegger, W. M. Wells, and A. F. Frangi, Eds. Cham: Springer International Publishing, 2015, pp. 234–241.
- [13] H. Zhao, O. Gallo, I. Frosio, and J. Kautz, "Loss functions for image restoration with neural networks," *IEEE Transactions on Computational Imaging*, vol. 3, no. 1, pp. 47–57, 2017.
- [14] A. Horé and D. Ziou, "Image quality metrics: Psnr vs. ssim," in *2010 20th International Conference on Pattern Recognition*, 2010, pp. 2366–2369.
- [15] R. Zhang, P. Isola, A. A. Efros, E. Shechtman, and O. Wang, "The unreasonable effectiveness of deep features as a perceptual metric," in *2018 IEEE/CVF Conference on Computer Vision and Pattern Recognition*, 2018, pp. 586–595.
- [16] C. Zhang and D. Lee, "Advancing nighttime object detection through image enhancement and domain adaptation," *Applied Sciences*, vol. 14, no. 18, 2024. [Online]. Available: <https://www.mdpi.com/2076-3417/14/18/8109>
- [17] Y. Yu, F. Chen, J. Yu, and Z. Kan, "Lmt-gp: Combined latent mean-teacher and gaussian process for semi-supervised low-light image enhancement," in *Computer Vision – ECCV 2024*, A. Leonardis, E. Ricci, S. Roth, O. Russakovsky, T. Sattler, and G. Varol, Eds. Cham: Springer Nature Switzerland, 2025, pp. 261–279.
- [18] R. M. H. Nguyen and M. S. Brown, "Why you should forget luminance conversion and do something better," in *2017 IEEE Conference on Computer Vision and Pattern Recognition (CVPR)*, 2017, pp. 5920–5928.
- [19] X. Guo, Y. Li, and H. Ling, "Lime: Low-light image enhancement via illumination map estimation," *IEEE Transactions on Image Processing*, vol. 26, no. 2, pp. 982–993, 2016.
- [20] X. Fu, D. Zeng, Y. Huang, X. Ding, and Y.-P. Zhang, "A weighted variational model for simultaneous reflectance and illumination estimation," in *Proceedings of the IEEE Conference on Computer Vision and Pattern Recognition*, 2016.
- [21] K.-F. Yang, X.-S. Zhang, and Y.-J. Li, "A biological vision inspired framework for image enhancement in poor visibility conditions," *IEEE Transactions on Image Processing*, vol. 29, pp. 1493–1506, 2020.
- [22] Z. Ying, G. Li, and W. Gao, "A bio-inspired multi-exposure fusion framework for low-light image enhancement," *arXiv preprint arXiv:1711.00591*, 2017.
- [23] C. W. Li, C. Li, and C. C. Loy, "Learning to enhance low-light image via zero-reference deep curve estimation," *IEEE Transactions on Pattern Analysis and Machine Intelligence*, vol. 44, no. 8, pp. 4225–4238, 2021.
- [24] Y. Jiang, X. Gong, D. Liu, Y. Cheng, C. Fang, X. Shen, J. Yang, P. Zhou, and Z. Wang, "Enlightengan: Deep light enhancement without paired supervision," *IEEE Transactions on Image Processing*, vol. 30, pp. 2340–2349, 2021.
- [25] C. Wei, W. Ren, W. Yang, and J. Liu, "Deep retinex decomposition for low-light enhancement," *arXiv preprint arXiv:1808.04560*, 2018.
- [26] Y. Zhang, J. Zhang, C. Xu, and X. Guo, "Kindling the darkness: A practical low-light image enhancer," in *ACM International Conference on Multimedia*, 2019, pp. 1632–1640.
- [27] S. W. Zamir, A. Arora, S. Khan, M. Hayat, F. S. Khan, and M.-H. Yang, "Learning enriched features for real image restoration and enhancement," in *European Conference on Computer Vision*, 2020, pp. 492–511.
- [28] Z. Wang, X. Cun, J. Bao, W. Zhou, D. Chen, and F. Wen, "Uformer: A general u-shaped transformer for image restoration," in *CVPR*, 2022, pp. 17 683–17 693.
- [29] S. W. Z. et al., "Restormer: Efficient transformer for high-resolution image restoration," in *CVPR*, 2022, pp. 5728–5739.
- [30] K.-F. Yang, C. Cheng, S.-X. Zhao, H.-M. Yan, X.-S. Zhang, and Y.-J. Li, "Learning to adapt to light," *International Journal of Computer Vision*, vol. 131, no. 4, pp. 1022–1041, 2023.
- [31] X. Lv, X. Dong, J. Yang, L. Zhao, B. Pu, Z. Jin, and Y. Zhang, "Low-light image enhancement with luminance duality," *Knowledge-Based Systems*, p. 114420, 2025.
- [32] H. Jiang, A. Luo, X. Liu, S. Han, and S. Liu, "Lightendiffusion: Unsupervised low-light image enhancement with latent-retinex diffusion models," in *European Conference on Computer Vision*. Springer, 2024, pp. 161–179.
- [33] S. Woo, J. Park, J.-Y. Lee, and I. S. Kweon, "Cbam: Convolutional block attention module," in *Computer Vision – ECCV 2018: 15th European Conference, Munich, Germany, September 8–14, 2018, Proceedings, Part VII*. Berlin, Heidelberg: Springer-Verlag, 2018, p. 3–19.
- [34] W. Yang, W. Wang, H. Huang, S. Wang, and J. Liu, "Sparse gradient regularized deep retinex network for robust low-light image enhancement," *IEEE Transactions on Image Processing*, vol. 30, pp. 2072–2086, 2021.